Front. Phys. 12(5), 124206 (2017)
DOI 10.1007/s11467-017-0702-x

RESEARCH ARTICLE

Cross-symmetry breaking of two-component discrete dipolar matter-wave solitons

Yong-Yao Li[1], Zhi-Wei Fan[2], Zhi-Huan Luo[2], Yan Liu[2], He-Xiang He[1], Jian-Tao Lü[1], Jia-Ning Xie[1], Chun-Qing Huang[1,†], Hai-Shu Tan[1]

[1] *School of Physics and Optoelectronic Engineering, Foshan University, Foshan 528000, China*
[2] *Department of Applied Physics, South China Agricultural University, Guangzhou 510642, China*
Corresponding authors. E-mail: † Chunqinghuang@qq.com
Received April 24, 2017; accepted June 21, 2017

We study the spontaneous symmetry breaking of dipolar Bose–Einstein condensates trapped in stacks of two-well systems, which may be effectively built as one-dimensional trapping lattices sliced by a repelling laser sheet. If the potential wells are sufficiently deep, the system is modeled by coupled discrete Gross–Pitaevskii equations with nonlocal self- and cross-interaction terms representing dipole–dipole interactions. When the dipoles are not polarized perpendicular or parallel to the lattice, the cross-interaction is asymmetric, replacing the familiar symmetric two-component solitons with a new species of cross-symmetric or -asymmetric ones. The orientation of the dipole moments and the interwell hopping rate strongly affect the shapes of the discrete two-component solitons as well as the characteristics of the cross-symmetry breaking and the associated phase transition. The sub- and super-critical types of cross-symmetry breaking can be controlled by either the hopping rate between the components or the total norm of the solitons. The effect of the interplay between the contact nonlinearity and the dipole angle on the cross-symmetry breaking is also discussed.

Keywords discrete matter-wave solitons, two-component systems, dipole–dipole interactions, cross-symmetry breaking

PACS numbers 42.65.Tg, 03.75.Lm, 05.45.Yv

1 Introduction

Dipolar Bose–Einstein condensates (BECs) composed of polar atoms and molecules are the subject of active and broad research in atomic and low-temperature physics. This type of BEC, which is dominated by anisotropic long-range magnetic or electric dipole–dipole interactions (DDIs), differs significantly from typical BECs, whose intrinsic dynamics is driven by isotropic contact interactions induced by s-wave scattering. Studies of dipolar BECs have produced many fascinating experimental and theoretical results, which have been summarized in reviews and references therein [1–3].

One important advantage of the dipolar BEC is its excellent tunability. In addition to the fact that the atomic or molecular dipoles can be polarized by external dc electric or magnetic fields, the sign of the DDI can be switched by a rotating ac field [4]. Moreover, atoms or molecules carrying field-induced magnetic or electric moments placed in spatially nonuniform fields are particularly interesting [5]. These tunable properties indicate the vast potential offered by dipolar BECs for fundamental and applied studies. One significant direction in these studies is the simulation of various phenomena that occur in a more complex form in other physical media, such as ferrofluidity [6–9], rotons [10–13], Faraday waves [14, 15], supersolids [16, 17], anisotropic superfluidity [18, 19] and anisotropic collapse [20–23], mesoscopic drops stabilized by quantum fluctuations [24–27], and others [28–32].

Another remarkable ramification is the use of collective nonlinear modes in dipolar BECs to create matter-wave solitons. This topic was originally introduced in nonlinear optics with nonlocal media [33–36]. A noteworthy finding is that DDIs can help stabilize multidimensional matter-wave solitons [37, 38]. Various forms of bright [39–44], dark [45–48], vortex [49, 50], and discrete [51–54] solitons were predicted in dipolar condensates. Very recently, stable two-dimensional (2D) solitons were predicted in a dipolar BEC with spin–orbit coupling [55–

*arXiv: 1708.01116.

© Higher Education Press and Springer-Verlag Berlin Heidelberg 2017

Frontiers of Physics

58]. It was demonstrated that the DDI can create solitons not only in BECs but in an ultracold bosonic gas of the Tonks–Girardeau type [59].

Very recently, dipolar matter-wave solitons were studied in a two-component discrete system [60]. A sketch of this system is displayed in Fig. 1(a). It was found that when the dipoles are not polarized perpendicular or parallel to the lattice, the cross-interaction, which is induced by the DDIs between two lines, is asymmetric [in Fig. 1(b), the left and right sides of the n-th lattice on the upper line feel attractive and repulsive DDIs, respectively, from the lower line]. This asymmetric cross-interaction gives rise to an asymmetric nonlocal cross-phase-modulation (XPM) term in the discrete Gross–Pitaevskii equation (GPE) and brings about a new type of symmetry, which is called cross-symmetry, in two-component discrete solitons [see Eq. (9) below]. Typically, when the dipole angle θ is near 35.3° [see Eq. (6) below], two types of cross-symmetry, on-site (the cross-symmetric axis is at a lattice site) and off-site (the cross-symmetry axis is at the midpoint between two sites) cross-symmetry, are induced by the asymmetric cross-interaction of the DDI. However, in a broad range of dipole angles, cross-symmetry breaking, which replaces the off-site cross-symmetry, was not discussed in this paper. The process of generating cross-asymmetry solitons from cross-symmetry solitons remains unclear.

The objective of the present work is to investigate spontaneous cross-symmetry breaking and the associated phase transition, also known as the symmetry-breaking bifurcation, of discrete solitons supported by the asymmetric cross-interaction (i.e., nonlocal asymmetric XPM) in two-component systems. Spontaneous symmetry breaking is generally a ubiquitous phenomenon that occurs in broad areas of nonlinear physics [61]. As solitons are an important nonlinear phenomenon, a natural subject of analysis is spontaneous symmetry breaking of solitons in symmetric systems. In particular, many theoretical and experimental results on this subject have been reported in optical and matter-wave nonlinear settings, where the symmetry is frequently provided by dual-core or double-well structures [62–65]. Symmetry breaking of solitons in systems with local nonlinearity has been studied in detail theoretically [66–76]; the systems include discrete systems, which are represented by parallel arrays of coupled waveguides [77, 78].

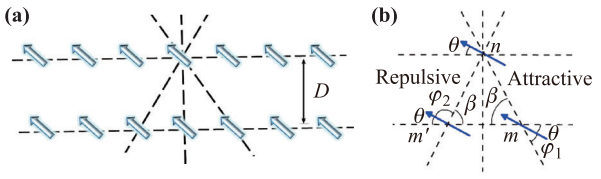

Fig. 1 **(a)** Dipoles in two-component discrete lattices are oriented by an external field in an arbitrary direction θ with respect to the horizontal (dashed) line. D is the distance between the two dashed lines. **(b)** Typical example of the contribution of the asymmetric nonlocal cross-interaction. In this sketch, if $\varphi_1 < 54.7°$ and $\varphi_2 > 54.7°$, the $m \leftrightarrow n$ and $m' \leftrightarrow n$ DDIs are attractive and repulsive, respectively, and produce the asymmetric nonlocal cross-interaction in this two-component system.

Spontaneous symmetry-breaking of solitons in systems with nonlocal nonlinear media is also an interesting problem, as the nonlocality strongly affects the outcome of spontaneous symmetry breaking when the nonlinearity strength exceeds a critical value [62]. To date, only few works have addressed this topic. In particular, the symmetry-breaking transformation of optical solitons in a dual-core coupler with nonlocal thermal nonlinearity was considered in Ref. [79]. Unlike the optical systems, the dipolar BEC dual-core setting exhibits not only intracore nonlocal nonlinearity but also an intercore DDI, which makes the situation essentially different. The differences were first shown in a model for an effectively one-dimensional (1D) dual-core coupler filled with a dipolar condensate [80]. In that work, sub- and supercritical symmetry breaking, (i.e., symmetry-breaking phase transitions of the first and second kinds, respectively) could be induced by competition between the inter- and intracore DDIs, respectively. However, the analysis in Ref. [80] considered a single polarization of the dipoles, namely, along the cores. In fact, an external magnetic field can polarize the dipoles in any direction, which offers an additional tool for working with dipolar systems. The aim of the present work is to explore the use of this degree of freedom to control the shape of discrete two-component solitons and the characteristics of the phase transition (symmetry-breaking bifurcation) in them. In particular, one of its essential feature is that, unless the dipole moments are oriented strictly perpendicular or parallel to the system's axis, the shapes of the solitons become irregular, i.e., spatially asymmetric, necessitating a modification of the definition of symmetry (and asymmetry) between the soliton's components, replacing it with cross-symmetry [see Eq. (9) below]. Moreover, spontaneous cross-symmetry breaking in discrete solitons supported by asymmetric cross-interactions has not been studied before.

The rest of the paper is structured as follows. The model is introduced in Section 2, and the cross-symmetry breaking in discrete two-component solitons controlled by the orientation of the dipoles is studied in Section 3. The paper is concluded in Section 4.

2 The model

We consider a chain of two-well systems into which a

dipolar BEC is loaded, as schematically shown in Fig. 1(a). It can be built as the usual quasi-1D lattice [81, 82], cut into a pair of parallel scalabilities by an additional repulsive (blue-detuned) laser sheet. Configurations with different orientations of the dipoles with respect to the lattice are also shown in Fig. 1(a).

In the tight-binding approximation [83–86] and using Wannier-like functions [51, 54, 87], the mean-field dynamics of the condensate in this system is governed by a two-component dimensionless discrete GPE [60]:

$$\begin{aligned} \mathrm{i}\frac{\mathrm{d}}{\mathrm{d}t}\tilde{\psi}_n &= -\frac{C}{2}(\tilde{\psi}_{n+1}+\tilde{\psi}_{n-1}) + \left[\sigma|\tilde{\psi}_n|^2 + \sum_{m\neq n}\left(F_{nm}|\tilde{\psi}_m|^2 + G_{nm}|\tilde{\phi}_m|^2\right)\right]\tilde{\psi}_n - J\tilde{\phi}_n, \\ \mathrm{i}\frac{\mathrm{d}}{\mathrm{d}t}\tilde{\phi}_n &= -\frac{C}{2}(\tilde{\phi}_{n+1}+\tilde{\phi}_{n-1}) + \left[\sigma|\tilde{\phi}_n|^2 + \sum_{m\neq n}\left(F_{nm}|\tilde{\phi}_m|^2 + G_{mn}|\tilde{\psi}_m|^2\right)\right]\tilde{\phi}_n - J\tilde{\psi}_n. \end{aligned} \tag{1}$$

Here, C and J are the coupling constants (determined by the respective hopping rates) along the lattice and between the wells, respectively; σ is the strength of the contact nonlinearity, and F_{nm} and G_{nm} are DDI kernels that account for the nonlocal self- and cross-interactions, respectively, in the coupled GPEs:

$$F_{nm} = \begin{cases} 0, & (m=n) \\ (1-3\cos^2\theta)/|m-n|^3 & (m\neq n) \end{cases}, \tag{2}$$

$$G_{nm} = \begin{cases} (1-3\sin^2\theta)/D^3 & (m=n) \\ \left[1-3\cos^2\varphi_1\right]/[D^2+(m-n)^2]^{3/2} & (m<n) \\ \left[1-3\cos^2\varphi_2\right]/[D^2+(m-n)^2]^{3/2} & (m>n) \end{cases}, \tag{3}$$

where D is the scaled interwell distance (vertical onsite distance), θ is the angle between the dipole orientation and horizontal axis [see Fig. 1(a)], $\varphi_1 = \beta - \theta$, and $\varphi_2 = \pi - (\beta + \theta)$ [see Fig. 1(c)], with $\beta \equiv \arccos\left(|m-n|/\sqrt{D^2+(m-n)^2}\right)$.

Typically, when $\theta = 0$ or $\pi/2$, G_{nm} is a symmetric matrix that satisfies $G_{nm} = G_{mn}$. For $0 < \theta < \pi/2$, G_{nm} is an asymmetric matrix satisfying $G_{nm} \neq G_{mn}$. This asymmetry is contributed by an asymmetric nonlocal cross-interaction [Fig. 1(b)]. In Ref. [60], we find that when $D < 0.7$, an off-site cross-symmetric soliton can be produced inside a narrow window near $\theta \approx 0.196\pi = 35.3°$ [see Eq. (6) below]. In this work, we consider the cross-symmetry breaking induced by the asymmetric G_{nm}; for convenience, we assume that the interwell distance D is equal to the horizontal distance between two adjacent lattice sites, i.e., $D = 1$, throughout the paper. In the following section, we will study the cross-symmetry breaking of a fundamental soliton from $\theta = 0$ to $\pi/2$ by numerical simulations. Recently, a configuration similar to Eq. (1) was considered as an Ising model with long-range interactions, which does not include horizontal hopping, i.e., with $C = 0$ [88].

Stationary states are searched for in the usual form,

$$(\tilde{\psi}_n, \tilde{\phi}_n) = (\psi_n, \phi_n)\mathrm{e}^{-\mathrm{i}\mu t}, \tag{4}$$

where (ψ_n, ϕ_n) are stationary wave functions, and μ is a real chemical potential. Two-component solitons are characterized by their total norm,

$$P = P_\psi + P_\phi \equiv \sum_{n=-N/2}^{n=N/2}\left(|\tilde{\psi}_n|^2 + |\tilde{\phi}_n|^2\right), \tag{5}$$

which is a dynamical invariant of Eq. (1). According to Ref. [51], if we assume that the width of the transverse confinement is ~ 5 μm, and the period of the optical lattice can be readily set to 5 μm, we conclude that $P = 1$ may correspond to ~ 1000 atoms in the condensates.

As mentioned above, for $\theta = 0$ or $\pi/2$, the matrix G_{nm} given by Eq. (3) is symmetric. Obviously, at $\theta = 0$, the *vertical* (also called interwell) interaction, i.e., the onsite DDI between condensate droplets trapped in the two wells, is repulsive, whereas the *horizontal* DDI within each sublattice is attractive. At $\theta = \pi/2$, the situation is the opposite; the onsite DDI in the two wells is attractive, whereas the horizontal DDI is repulsive.

When $0 < \theta < \pi/2$, the symmetry of the matrix is broken, which may contribute to an asymmetric nonlocal cross-interaction [Fig. 1(b)]. In the interval $\theta \in (0, \pi/2)$, there are two well-known special angles:

$$\theta_1 = \arcsin(1/\sqrt{3}) \approx 0.196\pi \approx 35.3°, \tag{6}$$

$$\theta_2 = \arccos(1/\sqrt{3}) \approx 0.304\pi \approx 54.7°. \tag{7}$$

When $\theta = \theta_1$, the vertical DDI vanishes, and the horizontal DDI remains attractive; when $\theta = \theta_2$, the horizontal DDI vanishes, and the vertical DDI is attractive. Even though the DDI between the two parallel lattices is anisotropic, its total effect remains attractive. Therefore, symmetry breaking may occur in the ground-state solution of the system. At $\theta = 0$ or $\pi/2$, the shapes of the ground-state solitons (which include symmetric and asymmetric ones with respect to the two components) that are produced by the system are spatially even, as mentioned above and shown below in Figs. 2(a1), (a2), and (d); i.e., they obey the spatial symmetry condition,

$$\phi_{-n} = \phi_n, \psi_{-n} = \psi_n. \tag{8}$$

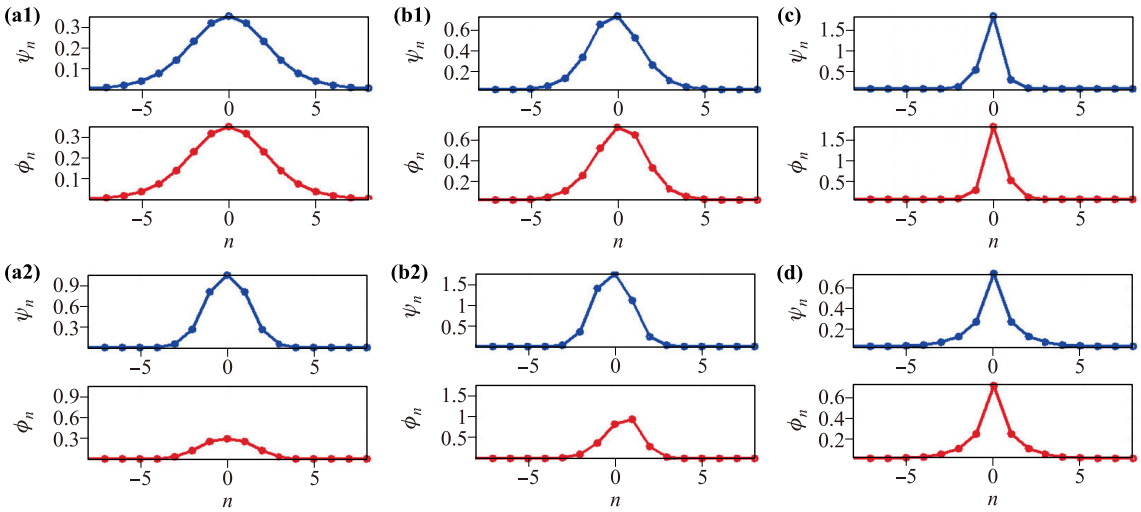

Fig. 2 Typical examples of discrete two-component solitons obtained by the imaginary-time method. **(a1, a2)** Symmetric and asymmetric solitons (with respect to the two components) for $(P, J, \theta) = (1, 1, 0)$ and $(3, 1, 0)$, respectively. **(b1, b2)** Symmetric and asymmetric solitons for $(P, J, \theta) = (3, 1, \arcsin(1/\sqrt{3}))$ and $(8, 1, \arcsin(1/\sqrt{3}))$, respectively. **(c, d)** Symmetric solitons for $(P, J, \theta) = (8, 1, \arccos(1/\sqrt{3}))$ and $(P, J, \theta) = (1.4, 1, \pi/2)$, respectively. Note that the spatial shape of the solitons is not even except when $\theta = 0$ in (a1) and (a2); see the text for details.

However, when $\theta \neq 0$ or $\pi/2$, G_{nm} is not a symmetric matrix [see Eq. (3)]; hence, the shapes of the two components are not spatially even. In particular, it is easy to see that, in this case, the symmetry condition with respect to the two components actually takes the form of the *cross-symmetry*, as clearly shown in Figs. 2(b1) and (c):

$$\phi_{-n} = \psi_n, \tag{9}$$

which is different from Eq. (8). To quantify the symmetry breaking of solitons in the system, we define the usual measure of the asymmetry between the two components in terms of their norms [cf. Eq. (5)]:

$$\eta = \frac{|P_\psi - P_\phi|}{P_\psi + P_\phi}. \tag{10}$$

In the following section, we study discrete solitons in this system and the cross-symmetry breaking between their two components (i.e., between the parallel sublattices) in the range $0 \leq \theta \leq \pi/2$ using numerical methods.

3 Spontaneous cross-symmetry breaking of two-component discrete solitons

3.1 System with $\sigma = 0$ (no contact interactions)

Ground-state discrete solitons, which always feature a site-centered *unstaggered* (smooth) shape [86] and may be both symmetric and asymmetric with respect to the two components, are obtained from Eq. (1) by the imaginary-time method (ITM) [89–91]. We arrange two types of initial guess for the ITM, symmetric and asymmetric, which refer to equal and unequal norm distributions, respectively. Before the symmetry-breaking bifurcation, both the symmetric and asymmetric initial guesses can generally produce only the symmetric state; however, after the symmetry-breaking bifurcation, the symmetric and asymmetric guesses produce symmetric and asymmetric states, respectively. The stabilities of the output symmetric or asymmetric states are verified by direct simulations of Eq. (1) realized by the four-step Runge–Kutta method. The stable state can propagate stably for a sufficiently long time. There are two types of symmetry-breaking bifurcation: sub- and supercritical. In the subcritical symmetry-breaking bifurcation (which is tantamount to the phase transition of the first kind), the system exhibits branches of asymmetric states that emerge as unstable ones, going at first backward from the bifurcation point and becoming stable after turning forward. Therefore, there is a small overlap (bistable) area of stable symmetry and asymmetry states; in this area, both the symmetric and asymmetric guesses can produce a stable output solution via the ITM. In the supercritical symmetry-breaking bifurcation (which is tantamount to the phase transition of the second kind), the asymmetric branches emerge as stable ones and immediately go in the forward direction.

To focus on the cross-symmetry breaking induced solely by the DDIs, here we first remove the contact nonlinearity; i.e., we set $\sigma = 0$ in Eq. (1) in this sec-

Frontiers of Physics

tion. Therefore, the remaining control parameters are the total norm P [see Eq. (5)], interwell hopping rate J in Eq. (1), and orientation angle θ. The horizontal hopping rate C is fixed as 1 throughout the paper.

Figure 2 shows typical examples of discrete solitons found for the dipole polarization angles $\theta = 0$, 0.196π, 0.304π, and $\pi/2$. For $\theta = 0$ and 0.196π, both stable symmetric and asymmetric solitons were found for smaller and larger values of P, respectively [Figs. 2(a1), (a2), (b1), and (b2)]. For $\theta = 0.304\pi$ and $\pi/2$, the system produces solely symmetric modes [Figs. 2(c) and (d)].

Figures 3(a) and (b) show the bifurcation diagrams of cross-symmetry breaking as plots of the asymmetry η, as defined in Eq. (10), versus P at fixed θ, and η versus θ at fixed P, for asymmetric discrete solitons at $J = 1$, when only the supercritical bifurcation diagram is found. Typical examples of solutions selected from stable and unstable branches in Fig. 3(a) are displayed in Fig. 4. To

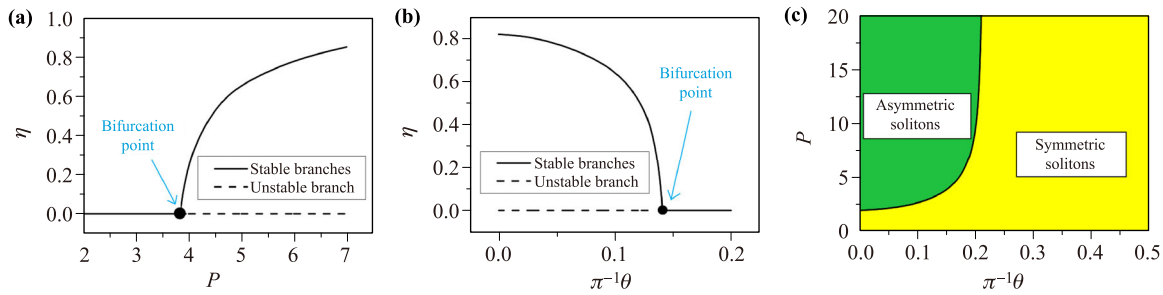

Fig. 3 **(a, b)** Symmetry-breaking bifurcation diagrams shown using $\eta(P)$ and $\eta(\theta)$ curves [Fig. 10]. In panels (a) and (b), $(J, \theta) = (1, \pi/6)$ and $(J, P) = (1, 3)$, respectively. Black solid dots are the bifurcation points; in panel (a), $P = 3.845$; in panel (b), $\theta = 0.141\pi$ (i.e., $\theta \approx 25.4°$). The solutions on the solid curves (stable branches) are stable, whereas those on the dashed lines (unstable branches) are unstable. **(c)** Black curve is the border between the yellow and green areas, which are populated by cross-symmetric and asymmetric solitons, respectively, in the (P, θ) plane, which is the locus of the bifurcation points for $J = 1$. The border is composed of supercritical symmetry-breaking bifurcation points. Here, $\sigma = 0$ (there are no contact interactions).

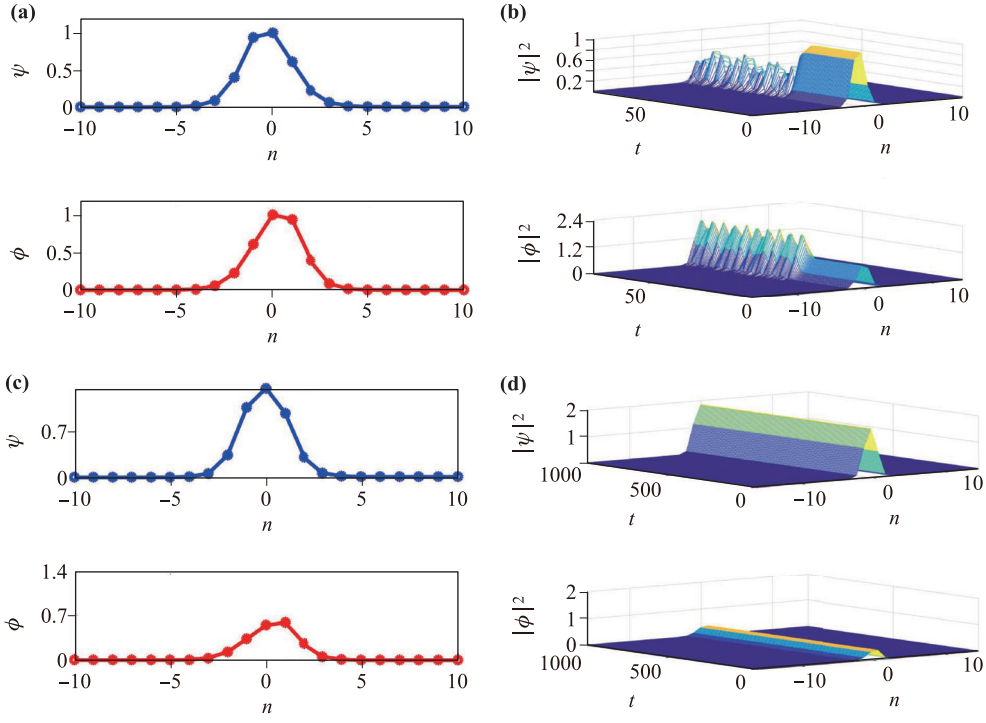

Fig. 4 Unstable (symmetric) soliton with $(P, J, \theta) = (5, 1, \pi/6)$, which is produced by the ITM with a symmetric input. **(b)** Direct simulation (real-time evolution) of the soliton solution in panel **(a)**. **(c)** Stable (asymmetric) soliton with the same controlled parameter as in panel (a), i.e., $(P, J, \theta) = (5, 1, \pi/6)$, which is produced by the ITM with an asymmetric input. **(d)** Direct simulation (real-time evolution) of the soliton solution in panel (c).

summarize these findings, the locus of bifurcation points is plotted in the (P, θ) plane in Fig. 3(c). The latter figure demonstrates that, at $\theta < 0.22\pi$ (i.e., $\theta < 39.6°$), increasing P leads to supercritical cross-symmetry-breaking bifurcation (i.e., the symmetry-breaking phase transition of the second kind). However, at $\theta > 0.22\pi$, cross-symmetry breaking does not occur at arbitrarily large values of norm P. Figure 3(c) also implies that, at fixed $P > 3.845$, one can induce supercritical cross-symmetry breaking by rotating the dipoles to smaller values of θ, i.e., closer to the system's axis. The fact that symmetry breaking never occurs for sufficiently large θ can be easily understood qualitatively. Indeed, with increasing θ, the attractive DDI in each component (along each sublattice), which drives the symmetry breaking, weakens, whereas the attraction between the sublattices, which obviously tends to suppress the symmetry breaking, strengthens. For this reason, $\theta = 0.22\pi$ is close to (slightly larger than) angle (6).

Figure 5 shows the bifurcation diagrams of the symme-

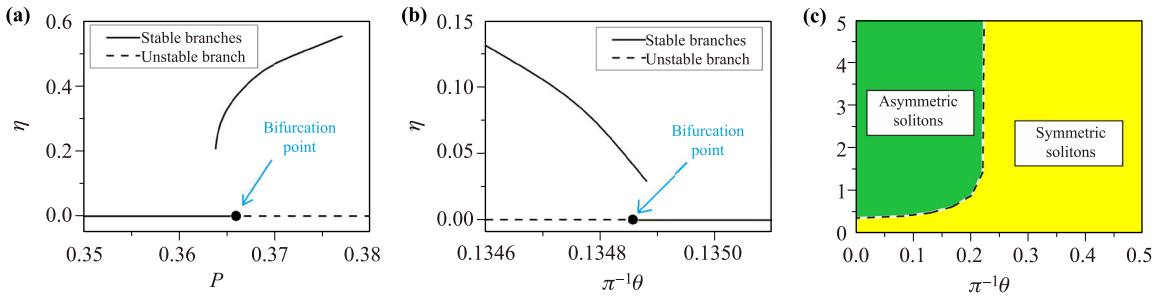

Fig. 5 The same as Fig. 3, but for a much weaker vertical (interwell) hopping rate, $J = 0.1$. In panels **(a)** and **(b)**, $\theta = 0$ and $P = 0.5$, respectively, are fixed. The bifurcation points are $P = 0.365$ in (a) and $\theta = 0.13488\pi$ (i.e., $\theta \approx 24.28°$) in (b). Backward-going curves, which must connect the bifurcation point with the stable asymmetric branches [92], are not shown here, as imaginary-time integration methods cannot produce these unstable solutions. **(c)** Subcritical symmetry-breaking bifurcation (*black dashed line*). Here and in Fig. 7 below, to clearly display the locus of the bifurcation points, we do not show a bistable area of overlap between the cross-symmetric and asymmetric solitons, as it is too narrow to be clearly shown.

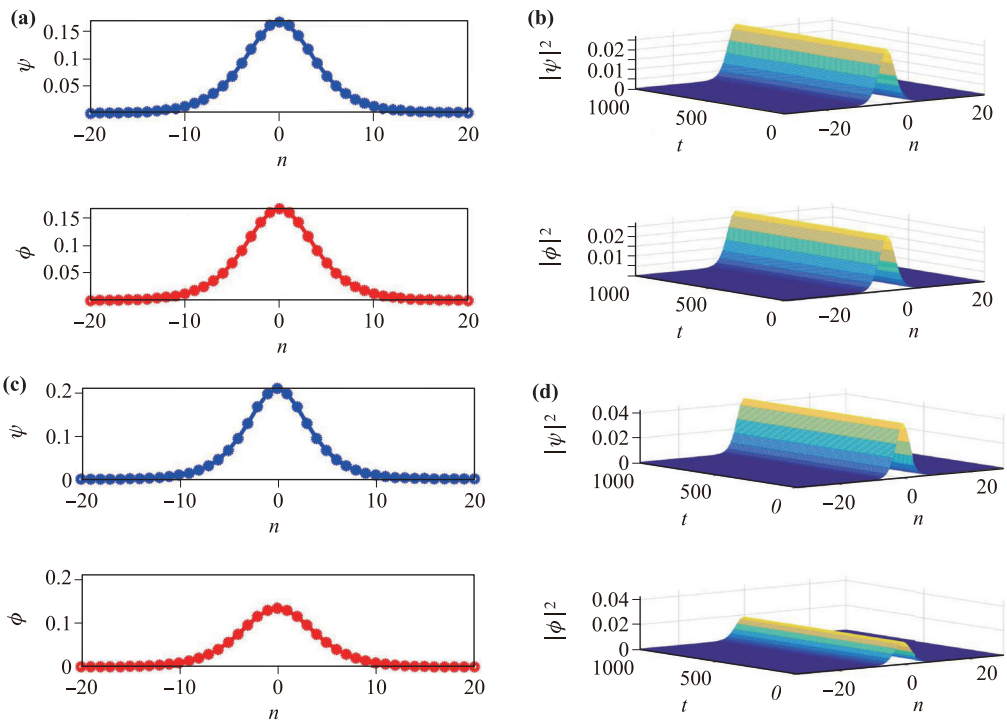

Fig. 6 Stable (symmetric) soliton with $(P, J, \theta) = (0.365, 0.1, 0)$, which is produced by the ITM with a symmetric input. **(b)** Direct simulation (real-time evolution) of the soliton solution in panel **(a)**. **(c)** Stable (asymmetric) soliton with the same controlled parameter as in panel (a), i.e., $(P, J, \theta) = (0.365, 0.1, 0)$, which is produced by the ITM with an asymmetric input. **(d)** Direct simulation (real-time evolution) of the soliton solution in panel (c).

try breaking for $J = 0.1$, i.e., for a much smaller interwell hopping rate. In this case, in contrast to that considered above for $J = 1$, only the subcritical cross-symmetry-breaking bifurcation (i.e., the symmetry-breaking phase transition of the first kind [92]) is found. Figure 6 shows typical examples of the bistable soliton in the area where the two stable branches overlap. Similar to the result for $J = 1$, at $\theta > 0.22\pi$, cross-symmetry breaking does not occur at arbitrarily large values of P. At $\theta < 0.22\pi$ and $P > 0.365$, either increasing P or downward rotation of θ from $\pi/2$ to 0 leads to the subcritical cross-symmetry-breaking bifurcation. Notice that the narrow intermediate unstable branches of asymmetric solitons, which connect the stable asymmetric branch and the bifurcation point on the symmetric branch, are missing, as the ITM does not converge to such unstable solutions [93].

The subcritical bifurcation gives rise to bistability, i.e., a region of coexistence of stable cross-symmetric and asymmetric discrete solitons [92]. This region is too narrow to appear clearly in Fig. 5(c) [a typical bistable case is shown below in Fig. 7(d)].

Figures 3 and 5 suggest that the type of symmetry-breaking bifurcation, i.e., the characteristics of the symmetry-breaking phase transition, can be switched by varying the parameters (P, J, θ). Figures 7(a), (b), and (c) demonstrate this possibility by displaying the loci of bifurcation points in cases where the bifurcation type indeed changes. This is shown in the (P, J) plane for $\theta = 0$ and 0.196π, as well as in the (P, θ) plane for $J = 0.45$ (for $\theta = 0$, the cross-symmetric solitons are replaced by the usual symmetric ones, as stated above). In these figures, solid and dashed lines designate supercritical and subcritical bifurcations, respectively, which are separated by the critical points (black dots).

To characterize the super- and subcritical symmetry-breaking bifurcations in further detail, we defined the size of the cross-symmetric soliton as

$$L = \frac{\left(\sum_n |\psi_n|^2\right)^2}{\sum_n |\psi_n|^4} \tag{11}$$

(because the cross-symmetric solitons obey the constraint $\psi_n = \phi_{-n}$ to define their size). Figure 8 shows L at the bifurcation point as a function of P and J for

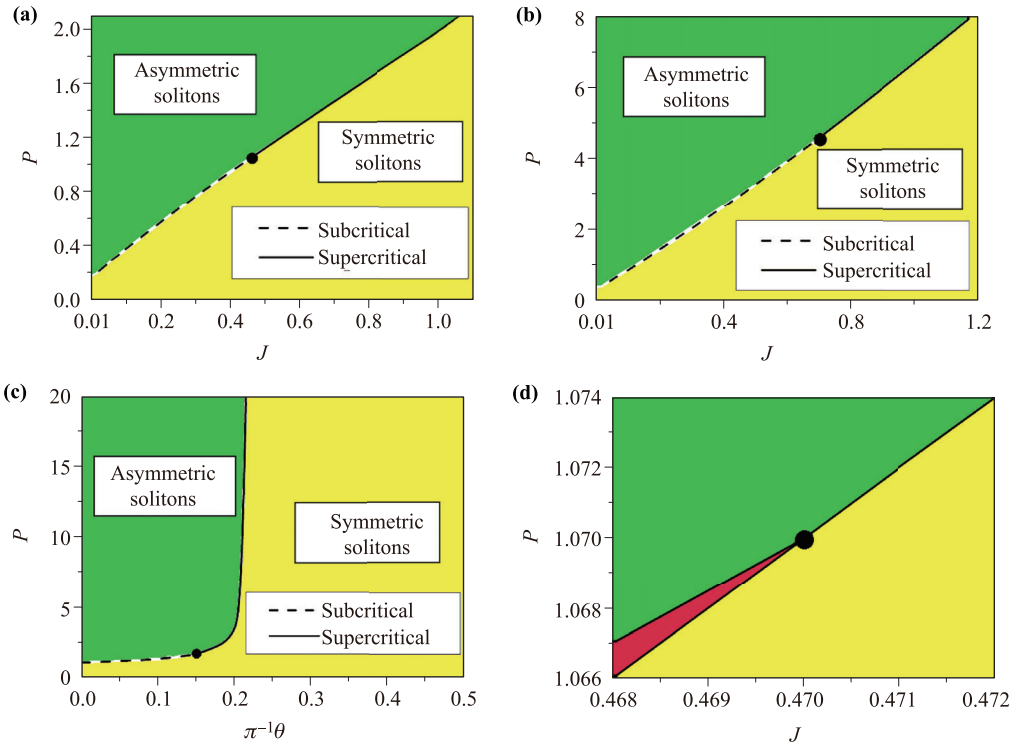

Fig. 7 **(a, b)** Loci of bifurcation points in the (J, P) plane for fixed values of the dipole orientation angle $\theta = 0$ and 0.196π, respectively. Here and in other figures, the solid and dashed lines designate supercritical and subcritical symmetry-breaking bifurcations, respectively. Critical points separating the super- and subcritical regions in panels (a) and (b) are $(P, J) = (1.07, 0.47)$ and $(4.59, 0.7)$, respectively. **(c)** Locus of bifurcation points in the (P, θ) plane for a fixed vertical (interwell) hopping rate, $J = 0.45$ [cf. Figs. 3(c) and 5(c)]. The critical point separating the sub- and supercritical regions is $(P, \theta) = (1.63, 0.15\pi)$. **(d)** Magnified view of region near the critical point (*black dot*) in panel (a). Red wedge is a narrow bistable area where stable cross-symmetric and asymmetric solitons coexist. The symmetry breaking in this area is of the subcritical type.

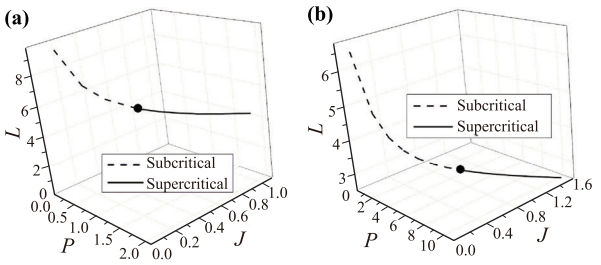

Fig. 8 Size of the (cross-)symmetric soliton at the bifurcation point, as defined in Eq. (11), versus P and J for $\theta = 0$ **(a)** and $\theta = 0.196\pi$ **(b)**. The critical points between the super- and subcritical segments in panels (a) and (b) are located at $L = 5.431$ and 3.021, respectively.

$\theta = 0$ and $\theta = \arcsin(1/\sqrt{3})$. The subcritical bifurcation tends to occur in broader solitons (with larger L), and the curvature of the $L(P, J)$ line is also larger when the bifurcation is subcritical.

Families of solitons are usually described by the dependence between the chemical potential μ and norm P. Figure 9 shows this dependence, supplemented by a panel showing μ as a function of the orientation angle θ at fixed P. The $\mu(P)$ dependence behaves somewhat differently in three regions: $\theta < 0.196\pi$, $0.196\pi < \theta < 0.304\pi$, and $\theta > 0.304\pi$ [see typical examples for these three cases in Figs. 9(a), (b), and (c), respectively]. Note that in all these panels, the Vakhitov–Kolokolov criterion, $\mathrm{d}\mu/\mathrm{d}P < 0$, holds; this is well-known as a necessary stability condition for a bright soliton supported by attractive nonlinearity [94–96]. Short flat segments with $\mu \approx -2$ in Fig. 9(c) belong not to solitons but to delocalized states, as the DDI cannot generate solitons in these regions. For $\theta < 0.192\pi$, the change in the slope of the $\mu(P)$ lines at $\mu \approx -2.7$ [dashed line in Fig. 9(a)] corresponds to the transition from cross-symmetric solitons to asymmetric ones. The smooth shape of $\mu(P)$ in the region $0.192\pi < \theta < 0.304\pi$ [Fig. 9(b)] is explained by the absence of symmetry breaking in this case [Fig. 3(c)]. The dependence of the μ value of the two-component soliton on the angle θ in this system is also studied. Figure 9(d) shows the μ value of the two-component soliton versus θ, namely, $\mu(\theta)$, for different values of P. This panel clearly shows that μ depends sensitively on θ. The relationship between μ and P shows different behavior in three regions: $\theta < 0.196\pi$, $0.196\pi < \theta < 0.304\pi$, and $\theta > 0.304\pi$.

3.2 System including contact interactions, $\sigma \neq 0$

To check the structural stability of the spontaneous symmetry-breaking phenomena against the inclusion of additional terms, we here address the contribution from the local nonlinearity, which is described by the coefficient σ in Eq. (1). This analysis also aims to establish a link between the present study and previous work that analyzed the spontaneous symmetry breaking in discrete two-component solitons created by on-site (local) interactions [77]. Figure 10 displays areas populated by cross-symmetric and asymmetric solitons in the (P, θ) plane for fixed $J = 1$. A comparison with the counterpart of this diagram at $\sigma = 0$ in Fig. 3(c) shows that the addition of the moderately strong repulsive ($\sigma > 0$) and attractive ($\sigma < 0$) contact interactions do not dramatically change the picture produced by the DDI. In particular, the symmetry-breaking bifurcation remains supercritical.

A qualitative change appears in the presence of a sufficiently strong attractive local nonlinearity, i.e., $\sigma < -2$; as Fig. 3(d) shows, in this case spontaneous symmetry breaking occurs at all values of θ, whereas at $\sigma > -2$ (including the case of $\sigma = 0$ considered above), symmetry breaking is absent in the interval $\theta_{\mathrm{cr}} < \theta \leq \pi/2$. In this region, the attractive contact nonlinearity is not enough to overcome the repulsive DDI along each sublattice, which suppresses the emergence of symmetry breaking. The corresponding dependence, $\theta_{\mathrm{cr}}(\sigma)$, which reaches $\pi/2$ and thus actually disappears at $\sigma \approx -2$, is shown in Fig. 11(a). In addition, Fig. 11(b) demonstrates that the onset of the symmetry-breaking bifurcation can be controlled by means of the contact interaction strength σ, which, in turn, may be tuned using the Feshbach resonance [97].

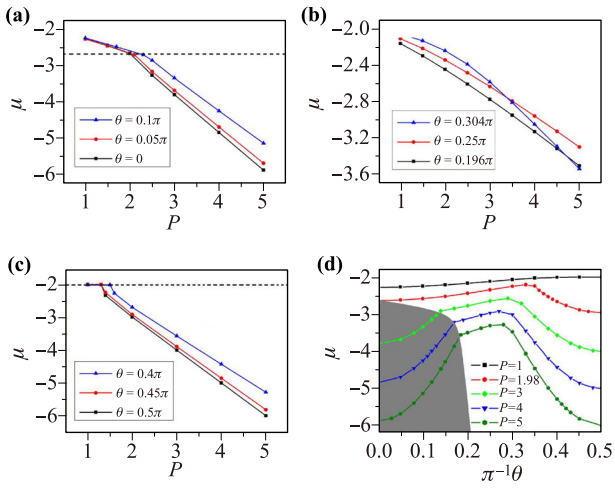

Fig. 9 **(a, b, c)** μ versus P for different fixed values of θ in three regions: $\theta < 0.196\pi$, $0.196\pi < \theta < 0.304\pi$, and $\theta > 0.304\pi$, respectively. In (a), the dashed line designates the transition to asymmetric solitons via symmetry breaking, whereas in (c), flat segments correspond to delocalized states in a region where solitons do not exist. In this figure, $J = 1$ and $\sigma = 0$. **(d)** Chemical potential of two-component discrete solitons, μ, versus θ at different fixed values of the total norm P. The solitons are asymmetric in the shaded area.

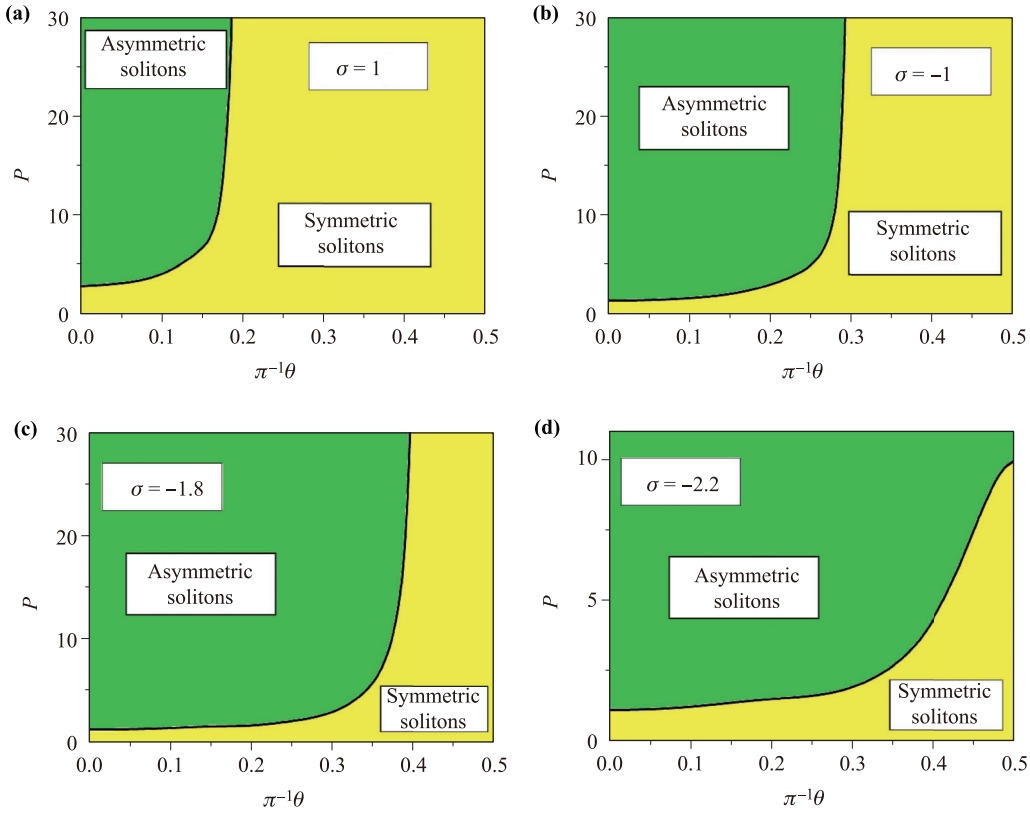

Fig. 10 Same as Fig. 3(c) ($J = 1$ in this figure and the following one), but in the presence of the contact interaction terms in Eq. (1) with strength $\sigma = 1$ (a), -1 (b), -1.8 (c), and -2.2 (d). In all cases, the symmetry-breaking bifurcation is supercritical. In panels (a), (b),and (c), symmetry breaking does not occur at $\theta > \theta_{\rm cr}$, with $\theta_{\rm cr} = 0.192\pi$, 0.3π, and 0.413π, respectively.

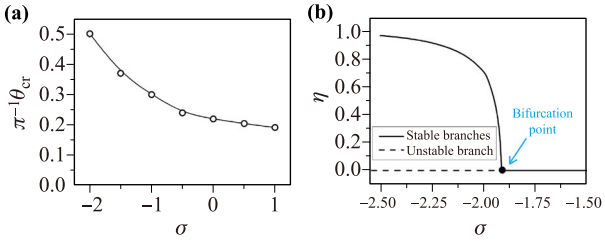

Fig. 11 **(a)** $\theta_{\rm cr}$, which is defined in the caption of Fig. 10, as a function of the strength $\sigma$of the attractive contact interaction. **(b)** Symmetry-breaking bifurcation diagram in the form of η vs. σ, where the other parameters are fixed: $(P, \theta) = (10, 0.4\pi)$. The bifurcation point is located at $\sigma = -1.914$.

4 Conclusion

We introduced a model of a dipolar BEC consisting of a chain of double-well potential traps. In the tight-binding approximation, it amounts to a system of two coupled discrete GPEs with long-range DDIs determined by the angle θ of the orientation of the dipoles with respect to the system's axis. Except for the limiting cases of $\theta = 0$ and $\theta = \pi/2$, the system gives rise to cross-symmetric discrete solitons, the main issue being the phase transitions (bifurcations) into spontaneous symmetry breaking of the cross-symmetric solitons. We found that the onset of spontaneous symmetry breaking, as well as the shape of the asymmetric solitons it generates, is controlled by the soliton's total norm P, rate of vertical (interwell) hopping J importantly, by θ. In particular, the supercritical symmetry-breaking bifurcation tends to switch to the subcritical type with decreasing θ and J.

A challenging issue may be an extension to a 2D discrete two-component system corresponding to dipolar BECs trapped in a deep 2D lattice cut into parallel sublattices by a repelling laser sheet. In that geometry, the DDI will be more complex than that in the 1D system. In particular, symmetry breaking may be expected not only in fundamental 2D solitons, but also in discrete solitary vortices [98].

Acknowledgements The authors appreciate the very useful discussion with Prof. Boris A. Malomed. This work was sup-

ported by the National Natural Science Foundation of China under Grant Nos. 11575063, 61471123, and 61575041, and the Natural Science Foundation of Guangdong Province under Grant No. 2015A030313639.

References

1. A. Griesmaier, Generation of a dipolar Bose–Einstein condensate, *J. Phys. B* 40(14), R91 (2007)
2. T. Lahaye, C. Menotti, L. Santos, M. Lewenstein, and T. Pfau, The physics of dipolar bosonic quantum gases, *Rep. Prog. Phys.* 72(12), 126401 (2009)
3. M. A. Baranov, Theoretical progress in many-body physics with ultracold dipolar gases, *Phys. Rep.* 464(3), 71 (2008)
4. S. Giovanazzi, A. Görlitz, and T. Pfau, Tuning the dipolar interaction in quantum gases, *Phys. Rev. Lett.* 89(13), 130401 (2002)
5. Y. Li, J. Liu, W. Pang, and B. A. Malomed, Matter-wave solitons supported by field-induced dipole–dipole repulsion with spatially modulated strength, *Phys. Rev. A* 88(5), 053630 (2013)
6. T. Lahaye, T. Koch, B. Fröhlich, M. Fattori, J. Metz, A. Griesmaier, S. Giovanazzi, and T. Pfau, Strong dipolar effects in a quantum ferrofluid, *Nature* 448(7154), 672 (2007)
7. H. Saito, Y. Kawaguchi, and M. Ueda, Ferrofluidity in a two-component dipolar Bose–Einstein condensate, *Phys. Rev. Lett.* 102(23), 230403 (2009)
8. H. Kadau, M. Schmitt, M. Wenzel, C. Wink, T. Maier, I. Ferrier-Barbut, and T. Pfau, Observing the Rosensweig instability of a quantum ferrofluid, *Nature* 530(7589), 194 (2016)
9. R. Richter and I. V. Barashenkov, Two-dimensional solitons on the surface of magnetic fluids, *Phys. Rev. Lett.* 94(18), 184503 (2005)
10. L. Santos, G. V. Shlyapnikov, and M. Lewenstein, Roton–Maxon spectrum and stability of trapped dipolar Bose–Einstein condensates, *Phys. Rev. Lett.* 90(25), 250403 (2003)
11. M. Klawunn, R. Nath, P. Pedri, and L. Santos, Transverse instability of straight vortex lines in dipolar Bose–Einstein condensates, *Phys. Rev. Lett.* 100(24), 240403 (2008)
12. R. M. Wilson, S. Ronen, J. L. Bohn, and H. Pu, Manifestations of the roton mode in dipolar Bose–Einstein condensates, *Phys. Rev. Lett.* 100(24), 245302 (2008)
13. D. Hufnagl, R. Kaltseis, V. Apaja, and R. E. Zillich, Roton–roton crossover in strongly correlated dipolar Bose–Einstein Condensates, *Phys. Rev. Lett.* 107(6), 065303 (2011)
14. R. Nath and L. Santos, Faraday patterns in two-dimensional dipolar Bose–Einstein condensates, *Phys. Rev. A* 81(3), 033626 (2010)
15. K. komy, R. Nath, and L. Santos, Faraday patterns in coupled one-dimensional dipolar condensates, *Phys. Rev. A* 86(2), 023620 (2012)
16. A. Bühler and H. P. Büchler, Supersolid phase in atomic gases with magnetic dipole interaction, *Phys. Rev. A* 84(2), 023607 (2011)
17. A. Maluckov, G. Gligoric, Lj. Hadžievski, B. A. Malomed, and T. Pfau, Stable periodic density waves in dipolar Bose–Einstein condensates trapped in optical lattices, *Phys. Rev. Lett.* 108(14), 140402 (2012)
18. C. Ticknor, R. M. Wilson, and J. L. Bohn, Anisotropic superfluidity in a dipolar Bose gas, *Phys. Rev. Lett.* 106(6), 065301 (2011)
19. A. A. Wood, B. H. J. McKellar, and A. M. Martin, Persistent superfluid flow arising from the He–McKellar–Wilkens effect in molecular dipolar condensates, *Phys. Rev. Lett.* 116(25), 250403 (2016)
20. P. M. Lushnikov, Collapse of Bose–Einstein condensates with dipole–dipole interactions, *Phys. Rev. A* 66, 051601 (2002)
21. D. C. E. Bortolotti, S. Ronen, J. L. Bohn, and D. Blume, Scattering length instability in dipolar Bose–Einstein condensates, *Phys. Rev. Lett.* 97(16), 160402 (2006)
22. C. Ticknor, N. G. Parker, A. Melatos, S. L. Cornish, D. H. J. O'Dell, and A. M. Martin, Collapse times of dipolar Bose–Einstein condensates, *Phys. Rev. A* 78, 061607 (2008)
23. T. Lahaye, J. Metz, B. Fröhlich, T. Koch, M. Meister, A. Griesmaier, T. Pfau, H. Saito, Y. Kawaguchi, and M. Ueda, d-wave collapse and explosion of a dipolar Bose–Einstein condensate, *Phys. Rev. Lett.* 101(8), 080401 (2008)
24. I. Ferrier-Barbut, H. Kadau, M. Schmitt, M. Wenzel, and T. Pfau, Observation of quantum droplets in a strongly dipolar Bose gas, *Phys. Rev. Lett.* 116(21), 215301 (2016)
25. K.-T. Xi and H. Saito, Droplet formation in a Bose–Einstein condensate with strong dipole–dipole interaction, *Phys. Rev. A* 93, 011604 (2016)
26. F. Wächtler and L. Santos, Quantum filaments in dipolar Bose–Einstein condensates, *Phys. Rev. A* 93, 061603 (2016)
27. D. Baillie, R. M. Wilson, R. N. Bisset, and P. B. Blakie, Self-bound dipolar droplet: A localized matter wave in free space, *Phys. Rev. A* 94, 021602 (2016)
28. M. Klawunn and L. Santos, Hybrid multisite excitations in dipolar condensates in optical lattices, *Phys. Rev. A* 80(1), 013611 (2009)
29. S. Müller, J. Billy, E. A. L. Henn, H. Kadau, A. Griesmaier, M. Jona-Lasinio, L. Santos, and T. Pfau, Stability of a dipolar Bose–Einstein condensate in a one-dimensional lattice, *Phys. Rev. A* 84(5), 053601 (2011)
30. R. M. Wilson and J. L. Bohn, Emergent structure in a dipolar Bose gas in a one-dimensional lattice, *Phys. Rev. A* 83(2), 023623 (2011)

31. K. Gawryluk, K. Bongs, and M. Brewczyk, How to observe dipolar Effects in spinor Bose–Einstein condensates, *Phys. Rev. Lett.* 106(14), 140403 (2011)
32. Q. Zhao and Q. Gu, Trapped Bose–Einstein condensates in synthetic magnetic field, *Front. Phys.* 10(5), 100306 (2015)
33. W. Królikowski, O. Bang, N. I. Nikolov, D. Neshev, J. Wyller, J. J. Rasmussen, and D. Edmundson, Modulational instability, solitons and beam propagation in spatially nonlocal nonlinear media, *J. Opt. B Quantum Semiclassical Opt.* 6(5), S288 (2004)
34. M. Peccianti and G. Assanto, Nematicons, *Phys. Rep.* 516(4–5), 147 (2012)
35. W. Królikowski and O. Bang, Solitons in nonlocal nonlinear media: Exact solutions, *Phys. Rev. E* 63(1), 016610 (2000)
36. S. Skupin, O. Bang, D. Edmundson, and W. Krolikowski, Stability of two-dimensional spatial solitons in nonlocal nonlinear media, *Phys. Rev. E* 73(6), 066603 (2006)
37. P. Pedri and L. Santos, Two-dimensional bright solitons in dipolar Bose–Einstein condensates, *Phys. Rev. Lett.* 95(20), 200404 (2005)
38. I. Tikhonenkov, B. A. Malomed, and A. Vardi, Anisotropic solitons in dipolar Bose–Einstein condensates, *Phys. Rev. Lett.* 100(9), 090406 (2008)
39. J. Cuevas, B. A. Malomed, P. G. Kevrekidis, and D. J. Frantzeskakis, Solitons in quasi-one-dimensional Bose–Einstein condensates with competing dipolar and local interactions, *Phys. Rev. A* 79(5), 053608 (2009)
40. F. Kh. Abdullaev, A. Gammal, B. A. Malomed, and L. Tomio, Bright solitons in quasi-one dimensional dipolar condensates with spatially modulated interactions, *Phys. Rev. A* 87(6), 063621 (2013)
41. M. Raghunandan, C. Mishra, K. Lakomy, P. Pedri, L. Santos, and R. Nath, Two-dimensional bright solitons in dipolar Bose–Einstein condensates with titled dipoles, *Phys. Rev. A* 92(1), 013637 (2015)
42. S. K. Adhikari and L. E. Young-S, Statics and dynamics of a binary dipolar Bose–Einstein condensate soliton, *J. Phys. B: At. Mol. Opt. Phys.* 47(1), 015302 (2014)
43. J. Huang, X. Jiang, H. Chen, Z. Fan, W. Pang, and Y. Li, Quadrupolar matter-wave soliton in two-dimensional free space, *Front. Phys.* 10(4), 100507 (2015)
44. G. Chen, Y. Liu, and H. Wang, Mixed-mode solitons in quadrupolar BECs with spin–orbit coupling, *Commun. Nonlinear Sci. Numer. Simul.* 48, 318 (2017)
45. R. Nath, P. Pedri, and L. Santos, Stability of dark solitons in three dimensional dipolar Bose–Einstein condensates, *Phys. Rev. Lett.* 101(21), 210402 (2008)
46. T. Bland, M. J. Edmonds, N. P. Proukakis, A. M. Martin, D. H. J. O'Dell, and N. G. Parker, Controllable nonlocal interactions between dark solitons in dipolar condensates, *Phys. Rev. A* 92(6), 063601 (2015)
47. K. Pawłowski and K. Rzążewski, Dipolar dark solitons, *New J. Phys.* 17(10), 105006 (2015)
48. M. J. Edmonds, T. Bland, D. H. J. O'Dell, and N. G. Parker, Exploring the stability and dynamics of dipolar matter-wave dark solitons, *Phys. Rev. A* 93(6), 063617 (2016)
49. V. M. Lashkin, Two-dimensional nonlocal vortices, multipole solitons, and rotating multisolitons in dipolar Bose–Einstein condensates, *Phys. Rev. A* 75(4), 043607 (2007)
50. I. Tikhonenkov, B. A. Malomed, and A. Vardi, Vortex solitons in dipolar Bose–Einstein condensates, *Phys. Rev. A* 78, 043614 (2008)
51. G. Gligorić, A. Maluckov, L. Hadžievski, and B. A. Malomed, Bright solitons in the one-dimensional discrete Gross–Pitaevskii equation with dipole–dipole interactions, *Phys. Rev. A* 78(6), 063615 (2008)
52. G. Gligorić, A. Maluckov, M. Stepič L. Hadžievski, and B. A. Malomed, Two-dimensional discrete solitons in dipolar Bose–Einstein condensates, *Phys. Rev. A* 81(1), 013633 (2010)
53. H. Chen, Y. Liu, Q. Zhang, Y. Shi, W. Pang, and Y. Li, Dipolar matter-wave solitons in two-dimensional anisotropic discrete lattices, *Phys. Rev. A* 93(5), 053608 (2016)
54. Z. Luo, Y. Li, W. Pang, and Y. Liu, Dipolar matter-wave soliton in one-dimensional optical lattice with tunable local and nonlocal nonlinearities, *J. Phys. Soc. Jpn.* 82(9), 094401 (2013)
55. Y. Xu, Y. Zhang, and C. Zhang, Bright solitons in a two-dimensional spin–orbit-coupled dipolar Bose–Einstein condensate, *Phys. Rev. A* 92(1), 013633 (2015)
56. X. Jiang, Z. Fan, Z. Chen, W. Pang, Y. Li, and B. A. Malomed, Two-dimensional solitons in dipolar Bose–Einstein condensates with spin–orbit-coupling, *Phys. Rev. A* 93(2), 023633 (2016)
57. Y. Li, Y. Liu, Z. Fan, W. Pang, S. Fu, and B. A. Malomed, Two-dimensional dipolar gap solitons in free space with spin–orbit coupling, *Phys. Rev. A* 95(6), 063613 (2017)
58. Y. Zhang, M. E. Mossman, T. Busch, P. Engels, and C. Zhang, Properties of spin–orbit-coupled Bose–Einstein condensates, *Front. Phys.* 11(3), 118103 (2016)
59. B. B. Baizakov, F. Kh. Abdullaev, B. A. Malomed, and M. Salerno, Solitons in Tonks–Girardeau gas with dipolar interactions, *J. Phys. At. Mol. Opt. Phys.* 42(17), 175302 (2009)
60. Z. Fan, Y. Shi, Y. Liu, W. Pang, Y. Li, and B. A. Malomed, Cross-symmetric dipolar-matter-wave solitons in double-well chains, *Phys. Rev. E* 95(3), 032226 (2017)
61. B. A. Malomed (Ed.), Spontaneous Symmetry Breaking, Self-Trapping, and Josephson Oscillations, Berlin: Springer, 2013

62. B. A. Malomed, Spontaneous symmetry breaking in nonlinear systems: An overview and a simple model, in: Nonlinear Dynamics: Materials, Theory and Experiments, edited by M. Tlidi and M. Clerc, Springer Proceedings in Physics Vol. 173, Berlin: Springer, 2016, pp 97–112
63. S. Trillo, E. M. Wright, G. I. Stegeman, and S. Wabnitz, Soliton switching in fiber nonlinear directional couplers, *Opt. Lett.* 13(8), 672 (1988)
64. S. R. Friberg, A. M. Weiner, Y. Silberberg, B. G. Sfez, and P. S. Smith, Femtosecond switching in a dual-core-fiber nonlinear coupler, *Opt. Lett.* 13(10), 904 (1988)
65. F. Kh. Abdullaev, R. M. Abrarov, and S. A. Darmanyan, Dynamics of solitons in coupled optical fibers, *Opt. Lett.* 14(2), 131 (1989)
66. E. M. Wright, G. I. Stegeman, and S. Wabnitz, Solitary-wave decay and symmetry-breaking instabilities in two-mode fibers, *Phys. Rev. A* 40(8), 4455 (1989)
67. C. Paré and M. Florjańczyk, Approximate model of soliton dynamics in all-optical couplers, *Phys. Rev. A* 41(11), 6287 (1990)
68. N. Akhmediev and A. Ankiewicz, Novel soliton states and bifurcation phenomena in nonlinear fiber couplers, *Phys. Rev. Lett.* 70(16), 2395 (1993)
69. P. L. Chu, B. A. Malomed, and G. D. Peng, Soliton switching and propagation in nonlinear fiber couplers: Analytical results, *J. Opt. Soc. Am. B* 10(8), 1379 (1993)
70. J. M. Soto-Crespo and N. Akhmediev, Stability of the soliton states in a nonlinear fiber coupler, *Phys. Rev. E* 48(6), 4710 (1993)
71. M. Matuszewski, B. A. Malomed, and M. Trippenbach, Spontaneous symmetry breaking of solitons trapped in a double-channel potential, *Phys. Rev. A* 75(6), 063621 (2007)
72. Y. J. Tsofe and B. A. Malomed, Quasisymmetric and asymmetric gap solitons in linearly coupled Bragg gratings with a phase shift, *Phys. Rev. E* 75(5), 056603 (2007)
73. S. K. Adhikari and B. A. Malomed, Two-component gap solitons with linear interconversion, *Phys. Rev. A* 79(1), 015602 (2009)
74. H. Sakaguchi and B. A. Malomed, Symmetry breaking of solitons in two-component Gross–Pitaevskii equations, *Phys. Rev. E* 83(3), 036608 (2011)
75. Y. Li, B. A. Malomed, M. Feng, and J. Zhou, Double symmetry breaking of solitons in one-dimensional virtual photonic crystals, *Phys. Rev. A* 83(5), 053832 (2011)
76. I. M. Merhasin, B. A. Malomed, and R. Driben, Transition to miscibility in a binary Bose–Einstein condensate induced by linear coupling, *J. Phys. B* 38(7), 877 (2005)
77. G. Herring, P. G. Kevrekidis, B. A. Malomed, R. Carretero-González, and D. J. Frantzeskakis, Symmetry breaking in linearly coupled dynamical lattices, *Phys. Rev. E* 76(6), 066606 (2007)
78. Y. Liu, Y. Guan, H. Li, Z. Luo, and Z. Mai, Nonlinear defect localized modes and composite gray and anti-gray solitons in one-dimensional waveguide arrays with dual-flip defects, *Opt. Commun.* 397, 105 (2017)
79. X. Shi, B. A. Malomed, F. Ye, and X. Chen, Symmetric and asymmetric solitons in a nonlocal nonlinear coupler, *Phys. Rev. A* 85(5), 053839 (2012)
80. Y. Li, J. Liu, W. Pang, and B. A. Malomed, Symmetry breaking in dipolar matter-wave solitons in dual-core couplers, *Phys. Rev. A* 87(1), 013604 (2013)
81. V. A. Brazhnyi and V. V. Konotop, Theory of nonlinear matter waves in optical lattices, *Mod. Phys. Lett. B* 18(14), 627 (2004)
82. O. Morsch and M. Oberthaler, Dynamics of Bose–Einstein condensates in optical lattices, *Rev. Mod. Phys.* 78(1), 179 (2006)
83. A. Trombettoni and A. Smerzi, Discrete solitons and breathers with dilute Bose–Einstein condensates, *Phys. Rev. Lett.* 86(11), 2353 (2001)
84. G. L. Alfimov, P. G. Kevrekidis, V. V. Konotop, and M. Salerno, Wannier functions analysis of the nonlinear Schrödinger equation with a periodic potential, *Phys. Rev. E* 66(4), 046608 (2002)
85. R. Carretero-González, and K. Promislow, Nonlinear excitations in arrays of Bose–Einstein condensates, *Phys. Rev. A* 66, 033610 (2002)
86. P. G. Kevrekidis, The Discrete Nonlinear Schrödinger Equation: Mathematical Analysis, Numerical Computations, and Physical Perspectives, Springer: Berlin and Heidelberg, 2009
87. F. K. Abdullaev, B. B. Baizakov, S. A. Darmanyan, V. V. Konotop, and M. Salerno, Nonlinear excitations in arrays of Bose–Einstein condensates, *Phys. Rev. A* 64(4), 043606 (2001)
88. Y. Li, W. Pang, J. Xu, C. Lee, B. A. Malomed, and L. Santos, Long-range transverse Ising model built with dipolar condensates in two-well arrays, *New J. Phys.* 19(1), 013030 (2017)
89. M. L. Chiofalo, S. Succi, and M. P. Tosi, Ground state of trapped interacting Bose–Einstein condensates by an explicit imaginary-time algorithm, *Phys. Rev. E* 62(5), 7438 (2000)
90. J. Yang and T. I. Lakoba, Accelerated imaginary-time evolution methods for the computation of solitary waves, *Stud. Appl. Math.* 120(3), 265 (2008)
91. J. Yang and T. I. Lakoba, Universally-convergent squared-operator iteration methods for solitary waves in general nonlinear wave equations, *Stud. Appl. Math.* 118(2), 153 (2007)
92. G. Iooss and D. D. Joseph, Elementary Stability Bifurcation Theory, New York: Springer, 1980
93. Y. Li, W. Pang, S. Fu, and B. A. Malomed, Two-component solitons with a spatially modulated linear coupling: Inverted photonic crystals and fused couplers, *Phys. Rev. A* 85(5), 053821 (2012)

94. M. Vakhitov and A. Kolokolov, Stationary solutions of the wave equation in a medium with nonlinearity saturation, *Radiophys. Quantum Electron.* 16(7), 783 (1973)

95. L. Bergé, Wave collapse in physics: principles and applications to light and plasma waves, *Phys. Rep.* 303(5–6), 259 (1998)

96. E. A. Kuznetsov and F. Dias, Bifurcations of solitons and their stability, *Phys. Rep.* 507(2–3), 43 (2011)

97. S. Inouye, M. R. Andrews, J. Stenger, H. J. Miesner, D. M. Stamper-Kurn, and W. Ketterle, Observation of Feshbach resonances in a Bose–Einstein condensate, *Nature* 392(6672), 151 (1998)

98. Z. Chen, J. Liu, S. Fu, Y. Li, and B. A. Malomed, Discrete solitons and vortices on two-dimensional lattices of PT-symmetric couplers, *Opt. Express* 22(24), 29679 (2014)